CUI, J., ZHANG, Y., YANG, F., CHANG, Y., DU, K., CHAN, A. and YAO, D. 2020. Seasonal fluxes and sources apportionment of dissolved inorganic nitrogen wet deposition at different land-use sites in the Three Gorges reservoir area. *Ecotoxicology and environmental safety* [online], 193, article 110344. Available from: https://doi.org/10.1016/j.ecoenv.2020.110344

Seasonal fluxes and sources apportionment of dissolved inorganic nitrogen wet deposition at different land-use sites in the Three Gorges reservoir area.

CUI, J., ZHANG, Y., YANG, F., CHANG, Y., DU, K., CHAN, A. and YAO, D.

2020

Ecotoxicology and Environmental Safety 193 (2020) 110344

Contents lists available at ScienceDirect

Ecotoxicology and Environmental Safety

journal homepage: www.elsevier.com/locate/ecoenv

Seasonal fluxes and sources apportionment of dissolved inorganic nitrogen wet deposition at different land-use sites in the Three Gorges reservoir area

Jian Cui[a,b,*], Yuanzhu Zhang[c], Fumo Yang[b], Yajun Chang[a], Ke Du[d], Andy Chan[e], Dongrui Yao[a,**]

[a] Institute of Botany, Jiangsu Province and Chinese Academy of Sciences, Nanjing Botanical Garden, Mem. Sun Yat-Sen, Nanjing, 210014, China
[b] Centre of Atmospheric Environment Research, Chongqing Institute of Green and Intelligent Technology, Chinese Academy of Sciences, Chongqing, 400714, China
[c] School of Geographical Sciences, Southwest University, Chongqing, 400715, China
[d] Department of Mechanical and Manufacturing Engineering, University of Calgary, Calgary, T2N 1N4, Canada
[e] Faculty of Engineering, University of Nottingham Malaysia Campus, Jalan Broga, Semenyih 43500, Selangor Darul Ehsan, Malaysia

A R T I C L E I N F O

Keywords:
Inorganic nitrogen
Nitrogen isotope
Wet deposition
Source apportionment
Three Gorges reservoir (TGR)

A B S T R A C T

To identify seasonal fluxes and sources of dissolved inorganic nitrogen (DIN) wet deposition, concentrations and $\delta^{15}N$ signatures of nitrate (NO_3^-) and ammonium (NH_4^+) in wet precipitation were measured at four typical land-use types in the Three Gorges reservoir (TGR) area of southwest China for a one-year period. Higher DIN fluxes were recorded in spring and summer and their total fluxes (averaged 7.58 kg N ha^{-1}) were similar to the critical loads in aquatic ecosystems. Significant differences of precipitation $\delta^{15}N$ were observed for NH_4^+-N between town and wetland sites in spring and between urban and rural sites in summer. For NO_3^--N, significant differences of precipitation $\delta^{15}N$ were observed between town and rural sites in spring and between urban and town sites in autumn, respectively. Quantitative results of NO_3^--N sources showed that both biomass burning and coal combustion had higher fluxes at the urban site especially in winter (0.18 ± 0.09 and 0.19 ± 0.08 kg N ha^{-1}), which were about three times higher than those at the town site. A similar finding was observed for soil emission and vehicle exhausts in winter. On the whole, DIN wet deposition averaged at 12.13 kg N ha^{-1} yr^{-1} with the urban site as the hotspot (17.50 kg N ha^{-1} yr^{-1}) and regional NO_3^--N fluxes had a seasonal pattern with minimum values in winter. The contribution to NO_3^--N wet deposition from biomass burning was 26.1 ± 14.1%, which is the second dominant factor lower than coal combustion (26.5 ± 12.6%) in the TGR area during spring and summer. Hence N emission reduction from biomass burning, coal combustion and vehicle exhausts should be strengthened especially in spring and summer to effectively manage DIN pollution for the sustainable development in TGR area.

1. Introduction

Anthropogenic nitrogen (N) emissions from energy development, rapid urban growth, and agricultural modernization contribute to the increasement of N deposition (Vet et al., 2014; Nanus et al., 2018; Vivanco et al., 2018; Wang et al., 2019a), which causes negative ecological effects, further to serious concern to global governments and scientists (Sutton et al., 2011; Boutin et al., 2017; Wang et al., 2019b; Liu and Du, 2020). Related abatement technologies and regulations have taken effect in hotpots of global N emission and deposition such as West Europe, the United States, and China (Xu et al., 2018; Theobald et al., 2018; Liu and Du, 2020), but there are still seasonal issues initiated by N emission and deposition such as haze in winter (Evanoski-Colea et al., 2017; Liu et al., 2019) and water eutrophication in summer (Oladosu et al., 2017; Ti et al., 2018; Wu et al., 2018). However, most studies of seasonal N deposition have been focused on fluxes and sources in agricultural and urban ecosystems, less attention was paid on seasonal risk assessments and source quantification in aquatic ecosystems (Leng et al., 2018; Matsumoto et al., 2019; Liu and Du, 2020). Moreover, water quality is inextricably bound to human health (Li et al., 2017; Schoen

* Corresponding author. Institute of Botany, Jiangsu Province and Chinese Academy of Sciences, Nanjing Botanical Garden, Mem. Sun Yat-Sen, Nanjing, 210014, China.
** Corresponding author.
E-mail addresses: jcui@cnbg.net (J. Cui), yaodongrui@cnbg.net (D. Yao).

https://doi.org/10.1016/j.ecoenv.2020.110344
Received 6 December 2019; Received in revised form 12 February 2020; Accepted 14 February 2020
Available online 21 February 2020

et al., 2017; Sanders-Demott et al., 2018). Thus, it is important to quantify the seasonal contribution of deposited N to water quality for developing emission control strategies, further to conserve regional public health.

Seasonal variations of N deposition can be significant due to seasonal variations in meteorological conditions (Cichowicz et al., 2017; Peng et al., 2017) and human activities, such as heating and smoking-meat during winter (Xue et al., 2016; Samek et al., 2020), straw burning in summer and autumn (Fu et al., 2017; Fushimi et al., 2017; Chen et al., 2018), and spring fertilization (Peng et al., 2017; Wang et al., 2019b). Because wet deposition is the chief form of deposited N, the current source tracking methods for N wet deposition reported in the literature were mainly based on GEOS-Chem (http://geos-chem.org) and SIAR model (Liu et al., 2017; Zhao et al., 2017; Xu et al., 2018; Cui et al., 2018). GEOS-Chem is driven by larger datasets including meteorology, emission source, underlying surface and so on, however, SIAR only needs N isotope ($\delta^{15}N$) signatures. More studies have shown that SIAR is a useful tool in identifying various source factors due to the unique value of $\delta^{15}N$ from different types of sources (Parnell et al., 2010; Liu et al., 2017; Cui et al., 2018).

The Three Gorges Reservoir (TGR) is located in southwest China and forms a total 58,000 km^2 reservoirs area, which is a typical fragile ecological zone. The industrial base in China has been shifting from the east to the west, where the city of Chongqing is the largest city for hosting the new industrial plants. Such industrial shift may increase the regional deposited N as reflected by the exceedances in the critical load of N deposition (Peng et al., 2017; Zhao et al., 2017; Cui et al., 2018). Seasonal pollution episodes are common in this region, such as hazy days in autumn and winter (Jiang et al., 2015; Liao et al., 2018; Li et al., 2019) and water eutrophication in spring to autumn (Yan et al., 2016; Gou et al., 2017; Zhou et al., 2019). In our two previous studies we measured dissolved inorganic N (DIN) concentrations and $\delta^{15}N$ signatures in precipitation at six sites covering four land-use types in the TGR area, and quantified annual N wet deposition and identified potential source factors (Leng et al., 2018; Cui et al., 2018). The same data set was used in this study, but we focused on exploring the seasonal N fluxes and $\delta^{15}N$ contents. The results would provide the needed knowledge for making targeted control policies for major sources in different seasons.

2. Methodology

2.1. Sampling sites

Six sampling sites were selected to represent four land-use types (urban, town, rural and wetland) in the TGR area of southwest China (Fig. 1A–B; Table S1). One urban site is in Wanzhou district (WZ) where there were some industrial plants (such as a lumber mill, a cement plant and a chemical plant) and farms feeding 500 chickens and 400 pigs. One town site is in Gaoyang town (GY) of Yunyang county. One wetland site is in Qukou town (QK) of Kaizhou district. The three rural sites are in Dede town (DD) and Houba town (HB) of Kaizhou district, and Renhe town (RH) of Yunyang county, respectively. Detailed descriptions of the sites and nearby emission sources were reported in Cui et al. (2018).

All the sampling sites are in the TGR area, where impounding begins in September and lasts until next April. In September or October, the water level in the TGR reaches to 135–175 m, which drowns a vast area

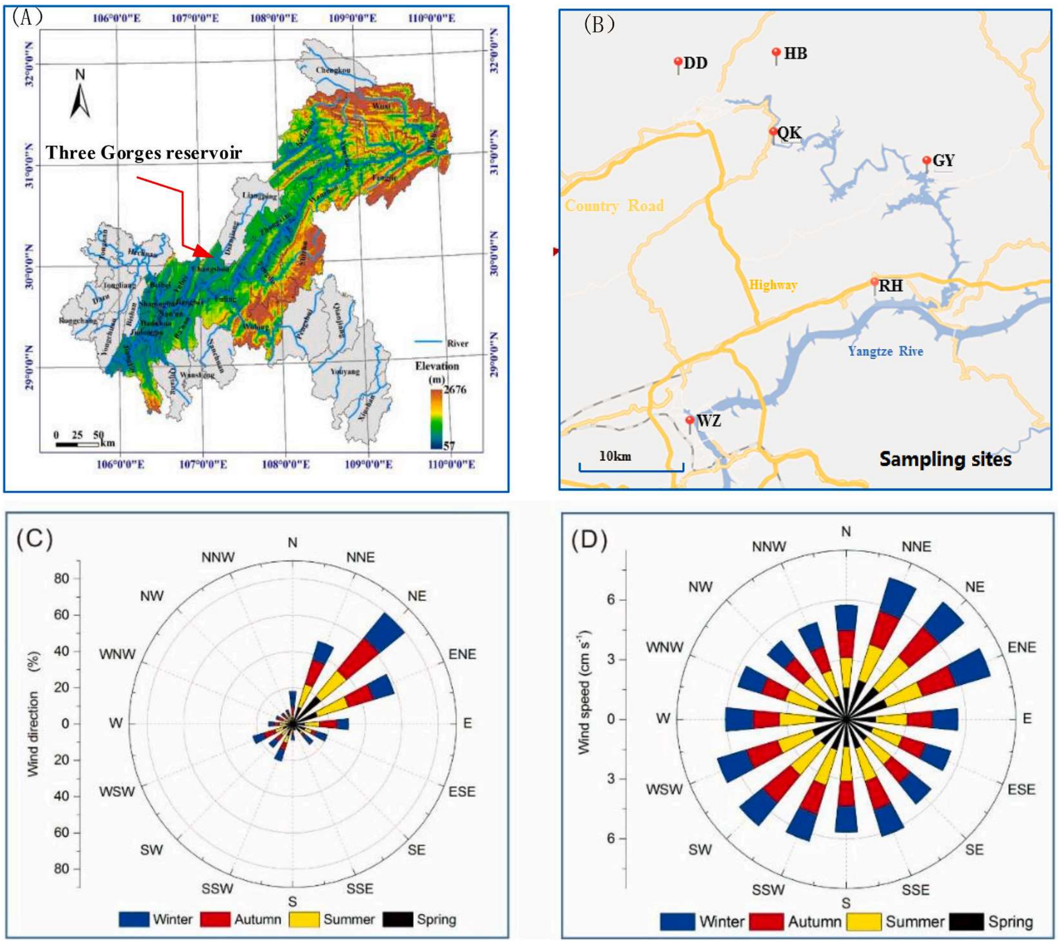

Fig. 1. The TGR of Chongqing (a) and location of the monitoring sites (b), and seasonal average wind direction (c) and speed (d) in 2016, respectively, of the TGR region.

of regional soils.

2.2. Sample collection and methods

A total of 457 precipitation samples were collected by auto-samplers (APS-3A, Changsha Xianglan Science Apparatus Ltd., China) and DIN concentrations of every rain event were determined by an ion chromatography (Dionex 600, Dionex Corp., USA). Monthly $\delta^{15}N$ values were determined from mixed samples in every month by an isotope ratio mass spectrometer (PT-IRMS, IsoPrime 100, IsoPrime Ltd., Germany) at each site, as detailed in earlier studies (Leng et al., 2018; Cui et al., 2018).

Based on the early study in our group, local $\delta^{15}N$–NH_3 sources especially for the biomass burning factor are limited (Table S2; Cui et al., 2018), and thus only seasonal sources of deposited NO_3^--N are discussed in this study and $\delta^{15}N$-NO_x values are presented in Table S2 and Fig. S1, respectively.

Fluxes of wet deposition N were calculated using equation (1):

$$F_i = (P_i \times C_i) / 100 \quad (1)$$

where F_i (kg N ha^{-1}), P_i (mm) and C_i (mg N L^{-1}) are the flux, rainfall amount and concentration of N during the *i*th rain event, *100* is the unit conversion factor. The monthly fluxes are shown in Fig. S2.

Based on the reported studies in the TGR area (Cui et al., 2018), there was a weak influence of precipitation amount, DIN concentrations and fluxes on the variation of $\delta^{15}N$ in precipitation. Thus the arithmetic averages of DIN fluxes and values of $\delta^{15}N$ at three sites of DD, HB and RH were regarded as the DIN fluxes and $\delta^{15}N$ values at the rural site in this study. These monthly DIN fluxes and seasonal $\delta^{15}N$ values were shown in Fig. S3 and Table S3, respectively.

Statistical analysis of seasonal or annual N fluxes and $\delta^{15}N$ values was conducted using one factor analysis of variance (ANOVA) in this study. The criterion for statistically significant difference was set as p values < 0.05 unless otherwise stated.

3. Results and discussion

3.1. Seasonal wet deposition of DIN

At all of the four sites, the summer had the largest rainfall (425.9–563.0 mm) while winter had the lowest rainfall (42.6–75.7 mm) (Fig. 2A). Such large seasonal variation in rainfall amounts partially caused the large seasonal variation in N wet deposition. For example, seasonal variations in NH_4^+-N wet deposition were up to a factor of 2.6 at urban site and 4.8 at wetland site, and for those in NO_3^--N, a factor of 2.0 at rural site and 3.5 at wetland site were observed for seasonal variation. The sum of NH_4^+-N and NO_3^--N (= DIN) also showed the smallest seasonal variation at urban site (a factor of 2.3) and the largest at wetland site (a factor of 4.8). On regional average (i.e., the average of the data for all the four sites), DIN wet deposition was the highest (3.72 kg N ha^{-1}) in spring and the lowest (1.33 kg N ha^{-1}) in winter, among these NH_4^+-N was from 0.93 kg N ha^{-1} (winter) to 2.78 kg N ha^{-1} (spring) and NO_3^--N from 0.40 kg N ha^{-1} (winter) to 0.95 kg N ha^{-1} (summer) (Fig. 2B). Significant differences in NO_3^--N, NH_4^+-N or DIN were found between winter and the other three seasons ($p < 0.05$; Fig. 2B).

Regarding site differences, annual DIN flux was remarkably higher at urban (17.50 kg N ha^{-1} yr^{-1}) than rural (10.29 kg N ha^{-1} yr^{-1}) or town (8.63 kg N ha^{-1} yr^{-1}) site ($p < 0.05$) (Table 1). No site differences were observed for annual NH_4^+-N (expect between urban and rural sites ($p < 0.05$)) or NO_3^--N flux among the four types ($p > 0.05$). Seasonally, there were no site differences for rainfall (Table 1; $p > 0.05$). Site differences were only significant in winter, with higher NO_3^--N, NH_4^+-N and DIN fluxes at urban site than town site ($p < 0.05$) and higher NH_4^+-N and DIN fluxes at urban site (1.73 and 2.37 kg N ha^{-1}) than rural (0.88 and 1.26 kg N ha^{-1}) or wetland (0.72 and 1.10 kg N ha^{-1}) site ($p < 0.05$). As for the three rural sites, site-differences were also observed but only in winter with higher NH_4^+-N and DIN fluxes at RH site than at the other two sites (Table S3; $p < 0.05$).

Compared with the critical loads of atmospheric N deposition in hydrosphere ecosystems (5–10 kg N ha^{-1} yr^{-1}), forest ecosystems (10–20 kg N ha^{-1} yr^{-1}) and farmland ecosystems (35–55 kg N ha^{-1} yr^{-1}) (Krupa, 2003; Fan and Huang, 2006), wet deposition fluxes of DIN in the study region (expect town site) exceeded the critical load in

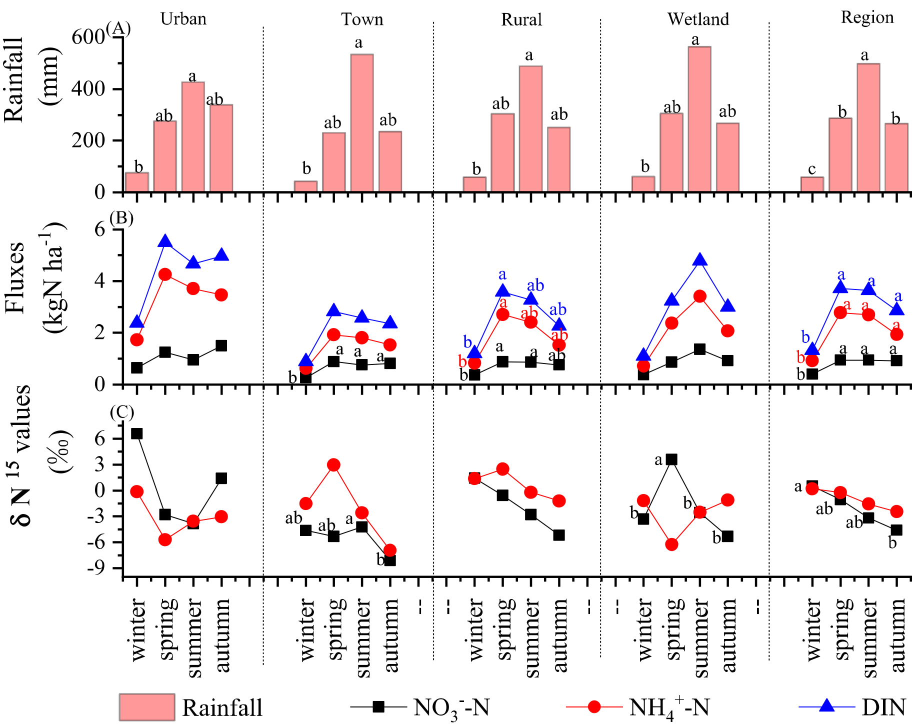

Fig. 2. Differences analysis and seasonal/regional variations of rainfall (A, unit: mm), wet deposition N fluxes (B, unit: kg N ha^{-1}) and precipitation $\delta^{15}N$ (C, unit: ‰) at urban, rural, town and wetland sites. On the bars and plots, different litter letters in the same color indicate the significance level ($p < 0.05$), and no lowercase letters or same lowercase letters indicate no significant level ($p > 0.05$). (For interpretation of the references to color in this figure legend, the reader is referred to the Web version of this article.)

Table 1
One-way ANOVA results are shown by letters and seasonal or annual rainfall, fluxes and $\delta^{15}N$ values for NH_4^+-N and NO_3^--N in rainwater samplers among four land-used types.

Season/ Year	Index	Land-used types			
		Urban	Town	Rural	Wetland
Winter	Rainfall (mm)	75.7a	42.6a	58.5a	61.2a
	NO_3^--N (kgN ha^{-1})	0.64a	0.26 b	0.38ab	0.39ab
	NH_4^+-N (kgN ha^{-1})	1. 73a	0.62 b	0.88 b	0.72 b
	DIN (kgN ha^{-1})	2.37a	0.89 b	1.26 b	1.10 b
	$\delta^{15}N$–NO_3^- (‰)	6.57a	−4.65a	−0.23a	1.70a
	$\delta^{15}N$–NH_4^+ (‰)	−0.16a	−1.55a	1.36a	−1.20a
Spring	Rainfall (mm)	275.0a	230.7a	303.5a	304.9a
	NO_3^--N (kgN ha^{-1})	1.25a	0.89a	0.88a	0.86a
	NH_4^+-N (kgN ha^{-1})	4.25a	1.93a	2.69a	2.37a
	DIN (kgN ha^{-1})	5.49a	2.82a	3.57a	3.23a
	$\delta^{15}N$–NO_3^- (‰)	−2.83ab	−5.35 b	1.79a	−3.70ab
	$\delta^{15}N$–NH_4^+ (‰)	−5.71ab	2.97a	1.86ab	−6.25 b
Summer	Rainfall (mm)	425.9a	532.8a	488.4a	563a
	NO_3^--N (kgN ha^{-1})	0.96a	0.76a	0.87a	1.36a
	NH_4^+-N (kgN ha^{-1})	3.71a	1.81a	2.31a	3.41a
	DIN (kgN ha^{-1})	4.67a	2.57	3.18a	4.78a
	$\delta^{15}N$–NO_3^- (‰)	−3.83a	−4.23a	−2.16a	−4.55a
	$\delta^{15}N$–NH_4^+ (‰)	−3.57 b	−2.59ab	−0.22a	−2.55ab
Autumn	Rainfall (mm)	338.9a	234.5a	251.0a	266.7a
	NO_3^--N (kgN ha^{-1})	1.50a	0.82a	0.77a	0.92a
	NH_4^+-N (kgN ha^{-1})	3.46a	1.53a	1.51a	2.07a
	DIN (kgN ha^{-1})	4.97a	2.35a	2.28a	2.99a
	$\delta^{15}N$–NO_3^- (‰)	1.41a	−8.15 b	−4.67ab	−6.34ab
	$\delta^{15}N$–NH_4^+ (‰)	−3.05a	−6.96a	−1.20a	−1.12a
Year	Rainfall (mm)	1115.5a	1040.6a	1101.4a	1195.8a
	NO_3^--N (kgN ha^{-1})	4.35a	2.74a	2.90a	3.53a
	NH_4^+-N (kgN ha^{-1})	13.15a	5.89 b	7.39ab	8.57ab
	DIN (kgN ha^{-1})	17.50a	8.63 b	10.29 b	12.10ab
	$\delta^{15}N$–NO_3^- (‰)	0.33a	−5.59 b	−1.32ab	−3.22ab
	$\delta^{15}N$–NH_4^+ (‰)	−3.12a	−2.49a	0.45a	−2.78a

Note: Different letters (such as a, b and c) in the same line at different land-used types in the same season indicate significant difference at 95% confidence level ($p < 0.05$), and the same letter indicates no significant difference at 95% confidence level ($p > 0.05$).

hydrosphere ecosystems. Earlier studies have shown that, in the TGR, water blooms often appeared in the spring-summer seasons (Holbach et al., 2015; Gou et al., 2017). During the same seasons, high DIN wet deposition was found in the study region with the total DIN fluxes ranged from 5.40 to 10.16 kg N ha^{-1}, which were similar to the critical loads of aquatic ecosystems, implying a seasonal threat to the aquatic ecosystem. A similar finding was observed in Jiaozhou Bay, North China (Xing et al., 2018). Thus, high DIN deposition found in the present study might have negative impacts on sensitive ecosystems such as the aquatic areas during spring and summer.

3.2. Seasonal sources of DIN wet deposition

3.2.1. NH_4^+-N sources

Looking at the four land-use types together, seasonal $\delta^{15}N$–NH_4^+ was in the range of −6.96‰ to +5.57‰ and no consistent seasonal trends were found (Fig. 2C). For different sites, significant differences for $\delta^{15}N$–NH_4^+ were observed between town (2.97‰) and wetland (−6.25‰) sites in spring and between rural (−0.22‰) and urban (−3.57‰) sites in summer, respectively (Table 1; $p < 0.05$).

Annual $\delta^{15}N$–NH_4^+ values in this study ranged from −3.12‰ to +0.45‰ (Table 1), which were similar to $\delta^{15}N$–NH_3 value (−3.4 ± 1.7‰) of vehicle exhausts (Table S2) while those in Guiyang (−10.6‰; Liu et al., 2017), Guangzhou (−7.3‰; Jia and Chen, 2010), Xiamen (−16.91‰; Yu et al., 2014) and Chengdu (−21.8‰; Du, 2012) were similar to $\delta^{15}N$–NH_3 value (−8.9 ± 4.1‰) of coal combustion (Table S2), implying a different dominant source for wet deposition NH_4^+-N between this study (vehicle exhausts) and other reported studies (coal combustion).

Early studies have shown that vehicle exhausts are an important source of NO_x emission. However, there is a long-standing and ongoing controversy regarding the contributions of vehicle and ship emissions to atmospheric NH_3 (Chang et al., 2016; Felix et al., 2017; Teng et al., 2017). In the US, vehicle exhausts accounted for 5%–12% of the national NH_3 emissions (Sutton et al., 2000; Kean et al., 2009). In China, Chang et al. (2016) estimated that vehicle-emitted NH_3 accounts for 12% of urban NH_3 emissions in Shanghai and pointed out that vehicle-emitted NH_3 might have potential implications for $PM_{2.5}$ pollution. Also, Tao et al. (2017) found that the vehicle exhausts factor contributed 27% to $PM_{2.5}$ in Guangzhou. In this study, we found that vehicle exhausts could be a leading contributor to NH_4^+-N wet deposition. The number of vehicles increased by ~300% in Chongqing municipality during 2006–2014 and those of the passengers and freighter in the study region (the Wan-Kai-Yun area), by 207%–365% and 284%–315%, respectively, during 2006–2012 (Table 2). Thus, attention should be paid for vehicle exhausts to reduce regional N pollution and protect ecosystem health.

3.2.2. NO_3^--N sources

Looking at the four land-use types together, seasonal $\delta^{15}N$–NO_3^- was in the range of −8.05‰ to +6.57‰ (Fig. 2C). Significant differences were found between winter (+0.49‰) and autumn (−4.61‰) ($p < 0.05$) for regional average $\delta^{15}N$–NO_3^-. For individual types, significant differences were only found between summer (−4.23‰) and autumn (−8.15‰) at town site, and between spring (+3.58‰) and the other seasons (−2.57‰ to −5.35‰) at wetland site. However, among different types, $\delta^{15}N$–NO_3^- in spring were respectively +1.79‰ and −5.35‰ at rural and town sites, and this difference was significant (Table 1; $p < 0.05$). Another significant difference was found for $\delta^{15}N$ –NO_3^- between urban (+1.41‰) and town (−8.15‰) sites in autumn ($p < 0.05$).

Based on monthly contributions of the four sources at the six individual sites (Fig. S4), annual and seasonal averages of percentage contribution to wet NO_3^--N deposition were calculated at four types and shown in Fig. 3. During spring and summer, soil emission, biomass burning, coal combustions and vehicle exhaustion contributed 22.2 ± 11.2%, 26.1 ± 14.1%, 26.5 ± 12.6%, and 25.2 ± 14.0% to deposited NO_3^--N, respectively. Significant differences ($p < 0.05$) were observed in the soil emission factor between town or wetland and rural sites in spring and between urban and town sites in autumn. The highest contributions of soil emission were found at town and wetland sites ($p < 0.05$) nearby the TGR where the reservoir storage and flash were usually during October to April and May to September, respectively, which could be attributed to the transformation and production of NO_x soil emission primarily mediated by nitrification and denitrification microbial activity (Fang et al., 2014; Xia et al., 2017). In the TGR region, Yu et al. (2018) found that N_2O emissions increased in the initial flooding period. Usually, there are some farming activities during the dry period in the TGR region, which also increased N_2O emissions (Fang et al., 2014; Li et al., 2016). In other regions, some studies have suggested that the flooding-drying conditions affected N_2O soil emissions in agricultural fields (Lu et al., 2014; Xia et al., 2017).

Also, significant differences were observed in the contributions of NO_3^--N wet deposition by biomass burning between urban (27.5 ± 14.5%) and wetland (25.3 ± 14.2%) sites in winter and between rural (27.1 ± 14.7%) and wetland (25.4 ± 14.1%) sites in spring (Fig. 3A–D; $p < 0.05$). As shown in Fig. 3, the highest contributions of biomass burning appeared at the rural site (26.4 ± 14.2%), which significantly differed from those at town and wetland sites (25.4 ± 13.7% and 25.2 ±

Table 2
Annual variations of business trucks (BT), business buses and cars (BBC), civil motor vehicles (CMV), transportation vessels (TV) (unit: 10^4 vehicle) in Chongqing municipality, and passenger transportation (unit: 10^6 persons) and freight transportation (unit: 10^6 tons) in Wanzhou, Kaizhou and Yunyang during 2006–2014.

Year	Chongqing municipality				Wanzhou		Kaizhou		Yunyang	
	BT	BBC	TMC	TV	PT	FT	PT	FT	PT	FT
2006	15.5	4.1	110.7	0.4	9.4	52.2	6.3	10.3	2.0	12.0
2007	17.6	5.0	132.0	0.4	12.9	65.7	6.6	12.4	2.6	16.0
2008	18.8	4.1	144.5	0.4	17.2	92.0	6.4	12.5	2.6	16.3
2009	20.0	4.3	162.8	0.4	19.7	144.9	5.9	15.7	2.8	18.7
2010	22.8	4.5	203.7	0.4	22.4	149.6	7.6	20.0	3.2	23.5
2011	26.0	4.8	276.0	0.4	28.6	152.6	10.6	23.8	3.8	28.7
2012	21.2	4.7	337.9	0.4	34.4	164.8	13.0	29.2	4.4	33.5
2013	23.5	5.0	389.9	0.4	nd.	nd.	nd.	nd.	nd.	nd.
2014	25.7	5.2	407.6	0.4	nd.	nd.	nd.	nd.	nd.	nd.

Note: "passenger transportation (PT) and freight transportation (FT), "nd." indicates on data. All of the data in the above table are from the Statistical Yearbook of Chongqing (2007–2015, Available online: http://www.cqtj.gov.cn/tjsj/sjzl/tjgb/201603/t20160311_423854.htm).

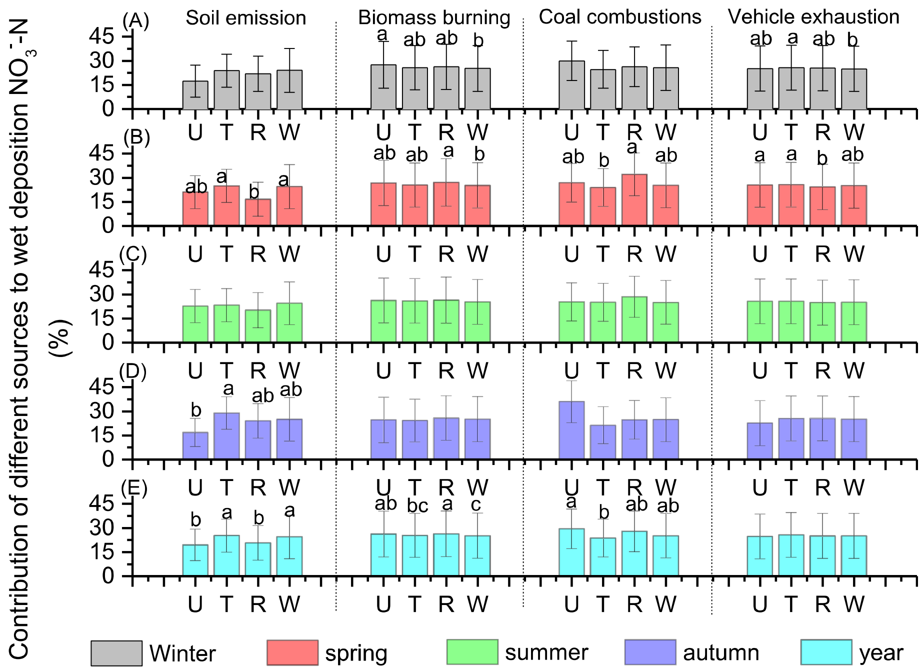

Fig. 3. Differences and seasonal and annual contributions (%) of four sources to NO_3^--N wet deposition between at four land-used types of urban (U), town (T), rural (R) and wetland (W). Different letters (such as a, b and c) on the bars at different types in the same season indicated significant difference at 95% confidence level ($p < 0.05$), and the same letter indicated no significant difference at 95% confidence level ($p > 0.05$). The same to Figs. 4 and 5.

14.1%; $p < 0.05$). This difference could be attributed to regional energy consumption and its seasonality. Cui et al. (2018) found that biomass energy consumption including firewood and crop straws was equivalent to 370.9 tons of standard coal, which accounted for 85.3% of rural energy consumption in the TGR region. In addition, weeds were burnt in fields before crop planting, and parts of crop straws were also burnt in open air after crop harvesting in spring and autumn (Peng et al., 2017), which led to higher contributions at rural site (Fig.3; 27.1 ± 14.7% in spring and 25.7 ± 13.8% in autumn).

Fig. 3 also shows that significant differences were observed in the coal combustion factor between rural and town sites in spring, and the vehicle exhausts factor between town and wetland sites in winter and between at urban or town and rural sites in spring, respectively ($p < 0.05$).

Based on the fluxes of the total NO_3^--N wet deposition on different land-use types (Fig. 2B) and the contributions from each source over the four seasons (Fig. 3), the source-specific NO_3^--N wet deposition fluxes were quantified for each of the four seasons (Fig. 4) and four land-use types (Fig. 5), respectively. As shown in Fig. 4, only in winter (expect coal combustion in autumn), there were significant differences in NO_3^--N fluxes from these four sources between urban and town sites (Fig. 4A–D; $p < 0.05$), implying a different NO_x emission intensity. On a whole year (Fig. 4E), NO_3^--N fluxes caused by biomass burning and coal combustion were 1.14 ± 0.62 and 1.28 ± 0.54 kg N ha^{-1} yr^{-1} at urban site, which significantly differed from those (0.69 ± 0.28 and 0.65 ± 0.32 kg N ha^{-1} yr^{-1}) at town site ($p < 0.05$), respectively. Thus, differences of regional NO_3^--N fluxes between the four types were from the two source factors of biomass burning and coal combustion especially in winter.

For the individual type, no seasonality was observed for NO_3^--N fluxes from all the four considered sources at urban and wetland sites ($p > 0.05$; Fig. 5A and D). At town and rural sites, NO_3^--N fluxes of all these four sources were the lowest in winter (Fig. 5B-C), which have the same seasonal pattern at the regional scale (Fig. 5E).

Furthermore, $\delta^{15}N$ values of emitted NOx are also dependent of fossil-fuel habitat, biomass location, and combustion temperature during the burning process (Redling et al., 2013; Felix et al., 2014). Redling et al. (2013) found that near-roadside NO_2 had an average $\delta^{15}N$–NO_2 of +1 ± 3.5‰, which was within the range of the value from biomass burning (−1±4.1‰, Table S2), implying that the percentage contributions of biomass burning calculated using the SIAR model might be

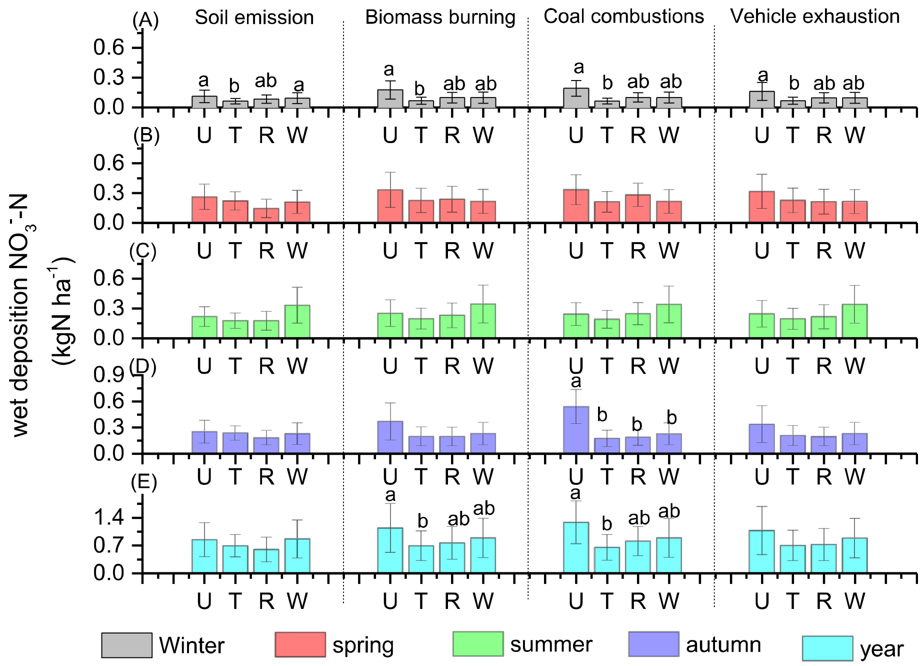

Fig. 4. Differences and seasonal and annual fluxes of NO_3^--N wet deposition between at the four land-used types of urban (U), town (T), rural (R) and wetland (W).

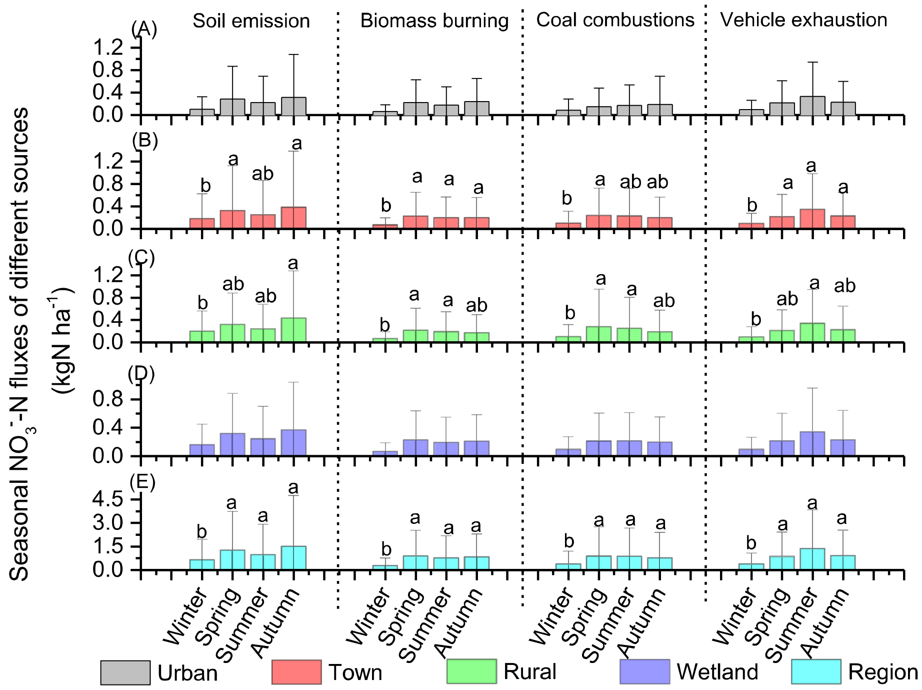

Fig. 5. Differences and seasonal fluxes of NO_3^--N wet deposition at the four land-used types and the whole region.

overestimated due to the possibility of partially including the contributions of the vehicle exhausts. Thus, more and detailed $\delta^{15}N$ values of atmospheric NO_x should be collected in order to accurately quantify the contributions from major sources in China.

4. Conclusions

In this study seasonal and annual DIN wet deposition flux and $\delta^{15}N$ signature were characterized, and relative contributions of dominant source factors to NO_3^--N fluxes were quantified. Regional DIN wet deposition ranged from 5.40 to 10.16 kg N ha^{-1} during spring to summer, which contributed to 58.1%–66.2% of the annual flux. Regional NH_4^+-N wet deposition flux was nearly two times higher than that of NO_3^--N. High DIN wet deposition observed in spring and summer could have potential detrimental effects on ecosystem health especially for aquatic ecosystems in the TGR area.

Combustion sources including biomass burning, coal combustion and vehicle exhausts could be dominant source factors to DIN wet deposition in this region. Nationwide NOx emission abatement strategies were initiated in 2012, but no control policies have been made for reducing NH_3 emissions. One measure for reducing biomass burning emissions could be prohibiting open-field burning of crop stalks in spring and autumn. Coal combustion should be controlled for decreasing N emissions at town and rural sites. Additional measures should be made to reduce vehicle exhausts emissions at town site.

CRediT authorship contribution statement

Jian Cui: Funding acquisition, Data curation, Investigation, Methodology, Resources, Validation, Writing – original draft, Writing – review & editing. **Yuanzhu Zhang:** Software, Formal analysis, Methodology, Visualization. **Fumo Yang:** Supervision, Data curation, Investigation, Project administration, Validation. **Yajun Chang:** Visualization, Writing – review & editing. **Ke Du:** Methodology, Visualization, Writing – review & editing. **Andy Chan:** Visualization, Writing – review & editing. **Dongrui Yao:** Supervision, Project administration, Writing – review & editing.

Acknowledgments

This work is partially founded by the National Natural Science Foundation of China (41571461; 41977333; 41901155) and Chongqing Science & Technology Commission (cstc2015jcyjBX0025). We appreciate our colleagues in the Centre of Atmospheric Environment Research, Chongqing Institute of Green and Intelligent Technology, Chinese Academy of Sciences for their assistance in the establishment of the sampling sites. Moreover, we would appreciate the editors and anonymous reviewers for their constructive comments and valuable suggestions for clarity of this manuscript.

Appendix A. Supplementary data

Supplementary data to this article can be found online at https://doi.org/10.1016/j.ecoenv.2020.110344.

References

Boutin, M., Corcket, E., Alard, D., Villar, L., Jimenez, J.J., 2017. Nitrogen deposition and climate change have increased vascular plant species richness and altered the composition of grazed subalpine grasslands. J. Ecol. 105, 1199–1209.

Chang, Y.H., Zou, Z., Deng, C.R., Huang, K., Collett, J.L., Lin, J., Zhuang, G.S., 2016. The importance of vehicle emissions as a source of atmospheric ammonia in the megacity of Shanghai. Atmos. Chem. Phys. 16, 3577–3594.

Chen, H.Y., Yin, S.S., Li, X., Wang, J., Zhang, R.Q., 2018. Analyses of biomass burning contribution to aerosol in Zhengzhou during wheat harvest season in 2015. Atmos. Res. 207, 62–73.

Cichowicz, R., Wielgosinski, G., Fetter, W., 2017. Dispersion of atmospheric air pollution in summer and winter season. Environ. Monit. Assess. 189 (12), 605.

Cui, J., Zhou, F.W., Gao, M., Zhang, L.Y., Zhang, L.M., Du, K., Leng, Q.M., Zhang, Y.Z., He, D.Y., Yang, F.M., Chan, A., 2018. A comparison of various approaches used in source apportionments for precipitation nitrogen in a mountain region of Southwest China. Envion. Pollut. Environ. Pollut. 241, 810–820.

Du, F., 2012. Inorganic Sulfur and Nitrogen Isotope Variation in Atmospheric Precipitation at Chengdu. Chengdu Univ. Tech., China. Chengdu (Master's thesis) (in Chinese).

Evanoski-Colea, A.R., Gebhart, K.A., Sivec, B.C., Zhou, Y., Capps, S.L., Daye, D.E., Prennic, A.J., Schurmanaasd, M.I., Sullivana, A.P., Lia, Y., Hande, J.L., Schichtel, B. A., Collett Jr., J.L., 2017. Composition and sources of winter haze in the Bakken oil and gas extraction region. Atmos. Environ. 156, 77–87.

Fan, H.B., Huang, Y.Z., 2006. Ecophysiological mechanism underlying the impacts of nitrogen saturation in terrestrial ecosystems on plants. J. Plant Physiol. Mol. Biol. 32 (4), 395–402 (in Chinese).

Fang, F., Sun, Z.W., Gao, H.T., Guo, J.S., Li, Z., 2014. N_2O emission and denitrification in the soils of water-level-fluctuation zone in the Three Gorges Reservoir area. Resour. Environ. Yangtze Basin 23 (2), 287–293 (in Chinese).

Felix, J.D., Elliott, E.M., Gay, D.A., 2017. Spatial and temporal patterns of nitrogen isotopic composition of ammonia at U.S. ammonia monitoring network sites. Atmos. Environ. 150, 434–442.

Felix, J.D., Elliott, E.M., Gish, T., Magrihang, R., Clougherty, J., Cambal, L., 2014. Examining the transport of ammonia emissions across landscapes using nitrogen isotope ratios. Atmos. Environ. 95, 563–570.

Fu, L., Wang, S.S., Wu, L.Z., 2017. Estimation of air pollutant emission from straw residues open burning in Henan Province. J. Agro-Environ. Sci. 36 (4), 808–816 (in Chinese).

Fushimi, A., Saitoh, K., Hayashi, K., Ono, K., Fujitani, Y., Villalobos, A.M., Shelton, B.R., Takami, K., Schauer, J.J., 2017. Chemical characterization and oxidative potential of particles emitted from open burning of cereal straws and rice husk under flaming and smoldering conditions. Atmos. Environ. 163, 118–127.

Gou, T., Ma, Q.L., Wang, Z.X., Wang, L., Yao, L.A., Xu, Z.C., Zhao, X.M., Liang, R.C., Lan, Y., 2017. Eutrophication and characteristics of cyanobecteria bloom in summer in Guishi Reseservoir. Environ. Sci. 38 (10), 4141–4150 (in Chinese).

Holbach, A., Bi, Y., Yuan, Y., Wang, L., Zheng, B., Norra, S., 2015. Environmental water body characteristics in a major tributary backwater of the unique and strongly seasonal Three Gorges Reservoir, China. Environ. Sci. Proc. Impacts 17, 1641–1653.

Jia, G.D., Chen, F.J., 2010. Monthly variations in nitrogen isotopes of ammonium and nitrate in wet deposition at Guangzhou, south China. Atmos. Environ. 44, 2309–2315.

Jiang, W.H., Liu, D., Chen, Y.H., Chen, D.Y., 2015. Temporal and spatial variations of haze days in Chongqing from 1980 to 2012. J. Arid Meteorol. 33 (4), 602–606 (in Chinese).

Kean, A.J., Littlejohn, D., Ban-Weiss, G.A., Harley, R.A., Kirchstetter, T.W., Lunden, M. M., 2009. Trends in on-road vehicle emissions of ammonia. Atmos. Environ. 43, 1565–1570.

Krupa, S.V., 2003. Effects of atmospheric ammonia (NH_3) on terrestrial vegetation: a review. Environ. Pollut. 124, 179–221.

Leng, Q.M., Cui, J., Zhou, F.W., Du, K., Zhang, L.Y., Fu, C., Liu, Y., Wang, H.B., Shi, G.M., Gao, M., Yang, F.M., He, D.Y., 2018. Wet-only deposition of atmospheric inorganic nitrogen and associated isotopic characteristics in a typical mountain area, southwestern China. Sci. Total Environ. 616–617, 55–63.

Li, P.Y., Feng, W., Xue, C.Y., Tian, R., Wang, S.T., 2017. Spatiotemporal variability of contaminants in lake water and their risks to human health: a case study of the Shahu lake tourist area, northwest China. Expos. Health 9, 213–225.

Li, R., Lei, L.G., Jiang, C.S., Chai, X.S., Huang, Z., Fang, Z.W., Hao, Q.J., 2016. Features and influencing factors of N_2O emissions from drawdown area in the Three Gorges Reservoir. Environ. Sci. 37 (7), 2721–2730 (in Chinese).

Li, Y., Xue, Y., Guang, J., de Leeuw, G., Self, R., She, L., Fan, C., Xie, Y., Chen, G., 2019. Spatial and temporal distribution characteristics of haze days and associated factors in China from 1973 to 2017. Atmos. Environ. 214, 116862.

Liao, T.T., Gui, K., Jiang, W.T., Wang, S.G., Wang, B.H., Zeng, Z.L., Che, H.Z., Wang, Y. Q., Sun, Y., 2018. Air stagnation and its impact on air quality during winter in Sichuan and Chongqing, southwestern China. Sci. Total Environ. 635, 576–585.

Liu, M.X., Huang, X., Song, Y., Tang, J., Cao, J.J., Zhang, X.Y., Zhang, Q., Wang, S.X., Xu, T.T., Kang, L., Cai, X.H., Zhang, H.S., Yang, F.M., Wang, H.B., Yu, J.Z., Lau, A.K. H., He, L.Y., Huang, X.F., Duan, L., Ding, A.J., Xue, L.K., Gao, J., Liu, B., Zhu, T., 2019. Ammonia emission control in China would mitigate haze pollution and nitrogen deposition but worsen acid rain. Proc. Natl. Acad. Sci. Unit. States Am. 116 (16), 7760–7765.

Liu, X.J., Du, E.Z., 2020. Atmospheric Reactive Nitrogen in China: Emission, Deposition and Environmental Impacts. Spring Nature Singapore Pte Ltd, Singapore.

Liu, X.Y., Xiao, H.W., Xiao, H.Y., Song, W., Sun, X.C., Zheng, X.D., Liu, C.Q., Koba, K., 2017. Stable isotope analyses of precipitation nitrogen sources in Guiyang, southwestern China. Environ. Pollut. 230, 486–494.

Lu, J., Liu, J.B., Sheng, R., Liu, Y., Chen, A.L., Wei, W.X., 2014. Effect of short-time drought process on denitrifying bacteria abundance and N_2O emission in paddy soil. Chin. J. Appl. Ecol. 25 (10), 2879–2884 (in Chinese).

Matsumoto, K., Sakata, K., Watanabe, Y., 2019. Water-soluble and water-insoluble organic nitrogen in the dry and wet deposition. Atmos. Environ. 218, 117022.

Nanus, L., Campbell, D.H., Lehmann, C.M.B., Mast, M.A., 2018. Spatial and temporal variation in sources of atmospheric nitrogen deposition in the Rocky Mountains using nitrogen isotopes. Atmos. Environ. 176, 110–119.

Oladosu, N.O., Abayomi, A.A., Olayinka, K.O., Alo, B.I., 2017. Wet nitrogen and phosphorus deposition in the eutrophication of the Lagos Lagoon, Nigeria. Environ. Sci. Pollut. Res. 24, 8645–8657.

Parnell, A.C., Inger, R., Bearhop, S., Andrew, L.J., 2010. Source partitioning using stable isotopes: coping with too much variation. PloS One 5, e9672.

Peng, Y., Zhou, F.W., Cui, J., Du, K., Leng, Q.M., Yang, F.M., Chan, A., Zhao, H.T., 2017. Impact of socio-economic and meteorological factors on reservoirs' air quality: a case in the Three Gorges Reservoir of Chongqing (TGRC), China over a ten-year period. Environ. Sci. Pollut. Res. 24 (19), 16206–16219.

Redling, K., Elliott, L., Bain, D., Sherwell, J., 2013. Highway contributions to reactive nitrogen deposition: reacing the fate of vehicular NOx using stable isotopes and plant biomonitors. Biogeochemistry 116 (1–3), 261–274.

Samek, L., Stegowski, Z., Styszko, K., Furman, L., Zimnoch, M., Skiba, A., Kistler, M., Kasper-Giebl, A., Rozanski, K., Konduracka, E., 2020. Seasonal variations of chemical composition of PM2.5 fraction in the urban area of Krakow, Poland: PMF source attribution. Air Qual. Atmos. Health 13, 89–96.

Sanders-Demott, R., Sorensen, P.O., Reinmann, A.B., Templer, P.H., 2018. Growing season warming and winter freeze-thaw cycles reduce root nitrogen uptake capacity and increase soil solution nitrogen in a northern forest ecosystem. Biogeochemistry 137 (3), 337–349.

Schoen, M.E., Xue, X.B., Wood, A., Hawkins, T.T., Garland, J., Ashbolt, N.J., 2017. Cost, energy, global warming, eutrophication and local human health impacts of community water and sanitation service options. Water Res. 109, 186–195.

Sutton, M.A., Dragosits, U., Tang, Y., Fowler, D., 2000. Ammonia emissions from non-agricultural sources in the UK. Atmos. Environ. 34, 855–869.

Sutton, M.A., Howard, C.M., Erisman, J.W., Billen, G., Bleeker, A., Grennfelt, P., Van Grinsven, H., Grizzetti, B., 2011. The European Nitrogen Assessment: Sources, Effects and Policy Perspectives. Cambridge University Press, U.N.

Tao, J., Zhang, L.M., Cao, J.J., Zhong, L.J., Chen, D.S., Yang, Y.H., Chen, D.H., Chen, L. G., Zhang, Z.S., Wu, Y.F., Xia, Y.J., Ye, S.Q., Zhang, R.J., 2017. Source apportionment of $PM_{2.5}$ at urban and suburban areas of the Pearl River Delta region, south China-with emphasis on ship emissions. Sci. Total Environ. 574, 1559–1570.

Teng, X.L., Hu, Q.J., Zhang, L.M., Qi, J.J., Shi, J.H., Xie, H., Gao, H.W., Yao, X.H., 2017. Identification of major sources of atmospheric NH_3 in an urban environment in northern China during wintertime. Environ. Sci. Technol. 51, 6839–6848.

Theobald, M.R., Vivanco, M.G., Aas, W., Andersson, C., Ciarelli, G., Couvidat, F., Cuvelier, K., Manders, A., Mircea, M., Pay, M.T., Tsyro, S., Adani, M., Bergström, R., Bessagnet, B., Briganti, G., Cappelletti, A., D'Isidoro, M., Fagerli, H., Mar, K., Otero, N., Raffort, V., Roustan, Y., Schaap, M., Wind, P., Colette, A., 2018. An evaluation of European nitrogen and sulfur wet deposition and their trends estimated by six chemistry transport models for the period 1990-2010. Atmos. Chem. Phys. 19, 379–405.

Ti, C.P., Gao, B., Luo, Y.X., Wang, S.W., Chang, S.X., Yan, X.Y., 2018. Dry deposition of N has a major impact on surface water quality in the Taihu Lake region in southeast China. Atmos. Environ. 190, 1–9.

Vet, R., Artz, R.S., Carou, S., Shaw, M., Ro, C.U., Aas, W., Baker, A., Bowersox, V.C., Dentener, F., Galy-Lacaux, C., Hou, A., Pienaar, J.J., Gillett, R., Cristina-Forti, M., Gromov, S., Hara, H., Khodzher, T., Mahowald, N.M., Nickovic, S., Rao, P.S.P., Reid, N.W., 2014. A global assessment of precipitation chemistry and deposition of sulfur, nitrogen, sea salt, base cations, organic acids, acidity and pH, and phosphorus. Atmos. Envion. 93, 3–100.

Vivanco, M.G., Theobald, M.R., García-Gómez, H., Garrido1, J.L., Prank, M., Aas, W., Adani, M., Alyuz, U., Andersson, C., Bellasio, R., Bessagnet, B., Bianconi, R., Bieser, J., Brandt, J., Briganti, G., Cappelletti, A., Curci, G., Christensen, J.H., Colette, A., Couvidat, F., Cuvelier, C., D'Isidoro, M., Flemming, J., Fraser, A., Geels, C., Hansen, K.M., Hogrefe, C., Im, U., Jorba, O., Kitwiroon, N., Manders, A., Mircea, M., Otero, N., Pay, M., Pozzoli, L., Solazzo, E., Tsyro, S., Unal, A., Wind, P., Galmarini, S., 2018. Modeled deposition of nitrogen and sulfur in Europe estimated by 14 air quality model systems: evaluation, effects of changes in emissions and implications for habitat protection. Atmos. Chem. Phys. 18, 10199–10218.

Wang, T.J., Gao, T.C., Zhang, H.S., Ge, M.F., Lei, H.C., Zhang, P.C., Zhang, P., Lu, C.S., Zhang, H., Zhang, Q., Liao, H., Kan, H.D., Feng, Z.Z., Zhang, Y.J., Qie, X.S., Cai, X.H., Li, M.M., Liu, L., Tong, S.R., 2019a. Atmospheric science study in China in recent 70 years: atmospheric physics and atmospheric environment. Sci. China Earth Sci. 62.

Wang, X.X., Cui, L.L., Yang, S.H., Xiao, J.L., Ding, Z.L., 2019b. Human-induced changes in Holocene nitrogen cycling in North China: an isotopic perspective from sedimentary pyrogenic material. Geophys. Res. Lett. 46, 4599–4608.

Wu, Y., Zhang, J., Liu, S., Jiang, Z., Arbi, I., Huang, X., Macreadie, P.I., 2018. Nitrogen deposition in precipitation to a monsoon-affected eutrophic embayment: fluxes, sources, and processes. Atmos. Environ. 182, 75–86.

Xia, S.M., Chen, J., Jiang, Y.L., Chen, L., Liu, H., Liu, L.J., 2017. Advances in nitrous oxide emission and its reduction in rice field. China Rice 23 (2), 5–9 (in Chinese).

Xing, J.W., Song, J.M., Yuan, H.M., Wang, Q.D., Li, X.G., Li, N., Duan, L.Q., Qu, B.X., 2018. Water-soluble nitrogen and phosphorus in aerosols and dry deposition in Jiaozhou Bay, North China: deposition velocities, origins and biogeochemical implications. Atmos. Res. 207, 90–99.

Xu, W., Liu, L., Cheng, M.M., Zhao, Y.H., Zhang, L., Pan, Y.P., Zhang, X.M., Gu, B.J., Li, Y., Zhang, X.Y., Shen, J.L., Lu, L., Luo, X.S., Zhao, Y., Feng, Z.Z., Collett Jr., J.F., Zhang, F.S., Liu, X.J., 2018. Spatial-temporal patterns of inorganic nitrogen air concentrations and deposition in eastern China. Atmos. Chem. Phys. 18, 10931–10954.

Xue, Y.F., Zhou, Z., Nie, T., Wang, K., Nie, L., Pan, T., Wu, X.Q., Tian, H.Z., Zhong, L.H., Li, J., Liu, H.J., Liu, S.H., Shao, P.Y., 2016. Trends of multiple air pollutants emissions from residential coal combustion in Beijing and its implication on improving air quality for control measures. Atmos. Environ. 142, 303–312.

Yan, H.Y., Zhang, X.R., Dong, J.H., Shang, M.S., Shan, K., Wu, D., Yuan, Y., Wang, X., Meng, H., Yuang, Y., Wang, G.Y., 2016. Spatial and temporal relation rule acquisition of eutrophication in Da'ning River based on rough set theory. Ecol. Indicat. 66, 180–189.

Yu, J.H., Zhang, J.Y., Chen, Q.W., Yu, W.Y., Hu, L.M., Shi, W.Q., Zhong, J.C., Yan, W.X., 2018. Dramatic source-sink transition of N_2O in the water level fluctuation zone of the Three Gorges Reservoir during flooding-drying process. Environ. Sci. Pollut. Res. 25, 20023–20031.

Yu, J.S., Wang, J., Zhao, L.J., Zhang, Y.S., 2014. Study on the source of sulfur and nitrogen in acid rain by using sulfur and nitrogen stable isotopic technology. J. Henan Normal Univ. (Nat. Sci.) 42 (4), 96–99 (in Chinese).

Zhao, Y.H., Zhang, L., Chen, Y.F., Liu, X.J., Xu, W., Pan, Y.P., Duan, L., 2017. Atmospheric nitrogen deposition to China: a model analysis on nitrogen budget and critical load exceedance. Atmos. Environ. 153, 32–40.

Zhou, B.T., Shang, M.S., Zhang, S., Feng, L., Liu, X.N., Wu, L., Feng, L., Shan, K., 2019. Remote examination of the seasonal succession of phytoplankton assemblages from time-varying trends. J. Environ. Manag. 246, 687–694.

Table S1 List of monitoring sites and their coordinates, elevations (m), number of samples, annual precipitation amount (mm yr^{-1}), and land use types.

Monitoring site	Coordinate	Elevation	Sample	Precipitation	Land type
Downtown,Wanzhou district (WZ)	N108.39°,E30.80°	300	91	1115.5	Urban
Dade, Kaizhou district (DD)	N108.36°,E31.22°	776	56	1243.3	Rural
Houbai, Kaizhou district (HB)	N108.56°,E31.24°	410	66	1132.6	Rural
Qukou, Kaizhou district (QK)	N108.56°,E31.15°	300	83	1195.8	Wetland
Gaoyang, Yunyang county (GY)	N108.68°,E31.10°	270	76	1040.6	Town
Renhe, Yunyang county (RH)	N108.62°,E31.04°	460	85	928.4	Rural

Table S2 Compiled $\delta^{15}N$ values (mean ± SD) of major NO_x and NH_3 emissions from different sources (Cui et al., 2018).

Sources	**N species**	**$\delta^{15}N$ / ‰**
Coal combustion	NO_x	+13.7±4.6
Mobile exhausts	NO_x	-7.25±7.8
Biomass burning	NO_x	+1.0±4.1
Biogenic soil emission	NO_x	-33.8±12.2
Coal combustion	NH_3	-8.9±4.1
Mobile exhausts	NH_3	-3.4±1.7
Biomass burning	NH_3	+12.0±na
Pig wastes	NH_3	-29.1±1.7
Human wastes	NH_3	-38.5±0.9
Chemical fertilizers	NH_3	-45.9±5.1

Table S3 Difference analysis and seasonal or annual rainfall, fluxes and $\delta^{15}N$ values for NH_4^+-N and NO_3^--N in rainwater samplers between at three rural sites.

Season/ Year	Indexes	DD	HB	RH
Winter	Rainfall (mm)	67.0a	60.5a	48.0 a
	NO_3^--N (kgN ha^{-1})	0.27a	0.31a	0.54 a
	NH_4^+-N(kgN ha^{-1})	0.62b	0.61b	1.25 a
	DIN (kgN ha^{-1})	0.90b	0.92b	1.79 a
	$\delta^{15}N$-NO_3^- (‰)	+6.44 a	-3.80 a	-3.34a
	$\delta^{15}N$-NH_4^+ (‰)	+2.06 a	+5.12 a	-3.10a
Spring	Rainfall (mm)	313.7 a	311.9 a	285.0a
	NO_3^--N (kgN ha^{-1})	1.10a	0.60a	0.94 a
	NH_4^+-N(kgN ha^{-1})	2.97a	2.56a	2.58 a
	DIN (kgN ha^{-1})	4.06a	3.16a	3.52 a
	$\delta^{15}N$-NO_3^- (‰)	-0.60 a	+2.60 a	+3.58a
	$\delta^{15}N$-NH_4^+ (‰)	+5.57 a	+2.84 a	-0.95a
Summer	Rainfall (mm)	562.3 a	503.9 a	398.9a
	NO_3^--N (kgN ha^{-1})	1.05a	0.73a	0.82 a
	NH_4^+-N(kgN ha^{-1})	3.15a	2.11a	1.95 a
	DIN (kgN ha^{-1})	4.21a	2.84a	2.77 a
	$\delta^{15}N$-NO_3^- (‰)	-5.37 a	+1.46 a	-2.57a
	$\delta^{15}N$-NH_4^+ (‰)	-0.15 a	-1.03 a	0.52 a
Autumn	Rainfall (mm)	300.3 a	256.3 a	196.5a
	NO_3^--N (kgN ha^{-1})	0.92a	0.64a	0.71 a

	NH_4^+-N(kgN ha^{-1})	2.07a	1.30a	1.17a
	DIN (kgN ha^{-1})	3.00a	1.94a	1.88a
	$\delta^{15}N$-NO_3^- (‰)	-5.28a	-3.96a	-5.35a
	$\delta^{15}N$-NH_4^+ (‰)	-0.84a	-0.15a	-2.70a
Year	Rainfall (mm)	1243.3a	1132.6a	928.4a
	NO_3^--N (kgN ha^{-1})	3.34a	2.28a	3.02a
	NH_4^+-N(kgN ha^{-1})	8.82a	6.58a	6.95a
	DIN (kgN ha^{-1})	12.16a	8.86a	9.97a
	$\delta^{15}N$-NO_3^- (‰)	-0.39a	-1.25a	-1.92a
	$\delta^{15}N$-NH_4^+ (‰)	+2.16a	+1.59a	-1.55a

Note: Different letters (such as a and b) in the same line at different land-use types in the same season indicated significant difference at 95% confidence level ($p<0.05$), and the same letter indicated no significant difference at 95% confidence level ($p>0.05$).

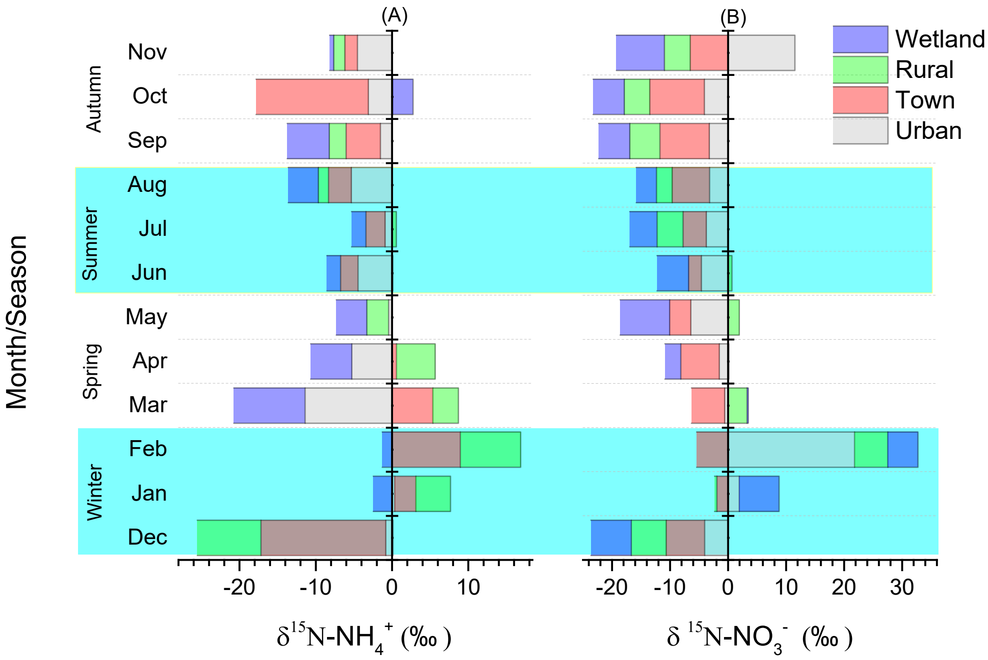

Fig.S1 Monthly and seasonal variations of δ^{15}N values for NH_4^+-N and NO_3^--N in rainwater among four land-used types.

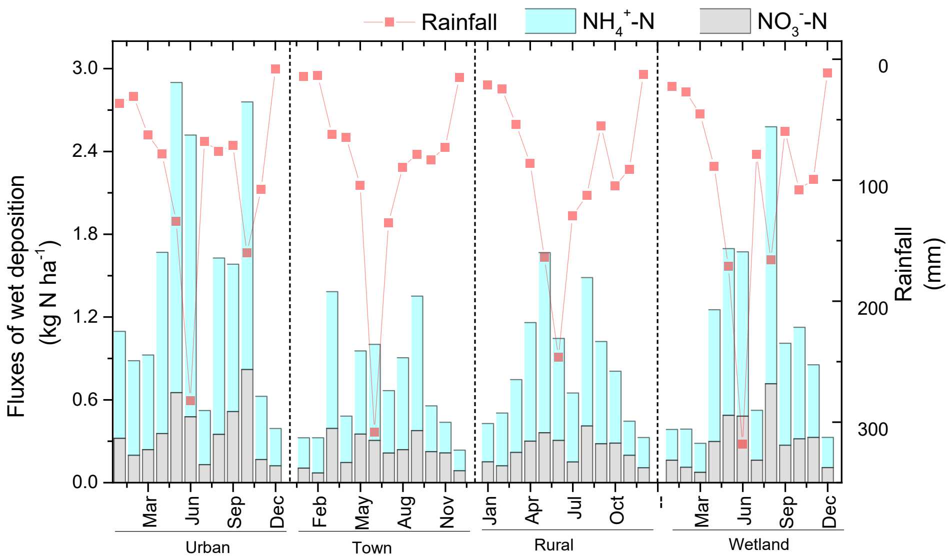

Fig.S2 Monthly variations of rainfall and fluxes of wet deposition N forms at different land-use types.

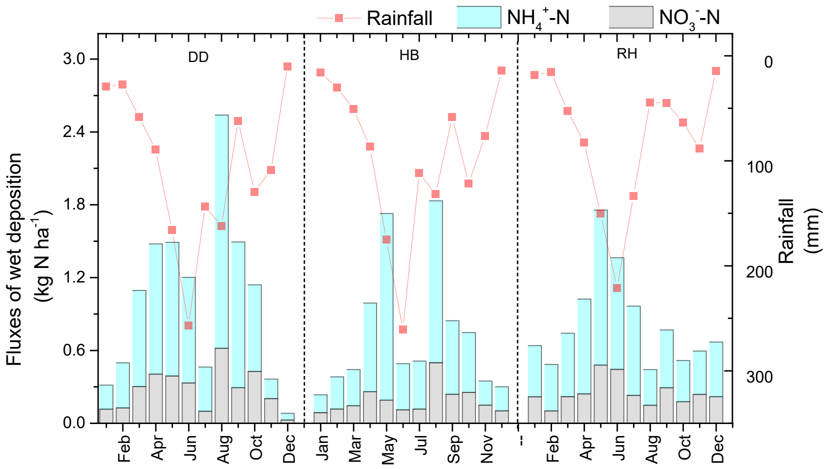

Fig.S3 Monthly variations of rainfall and fluxes of N forms in wet deposition at three rural sites

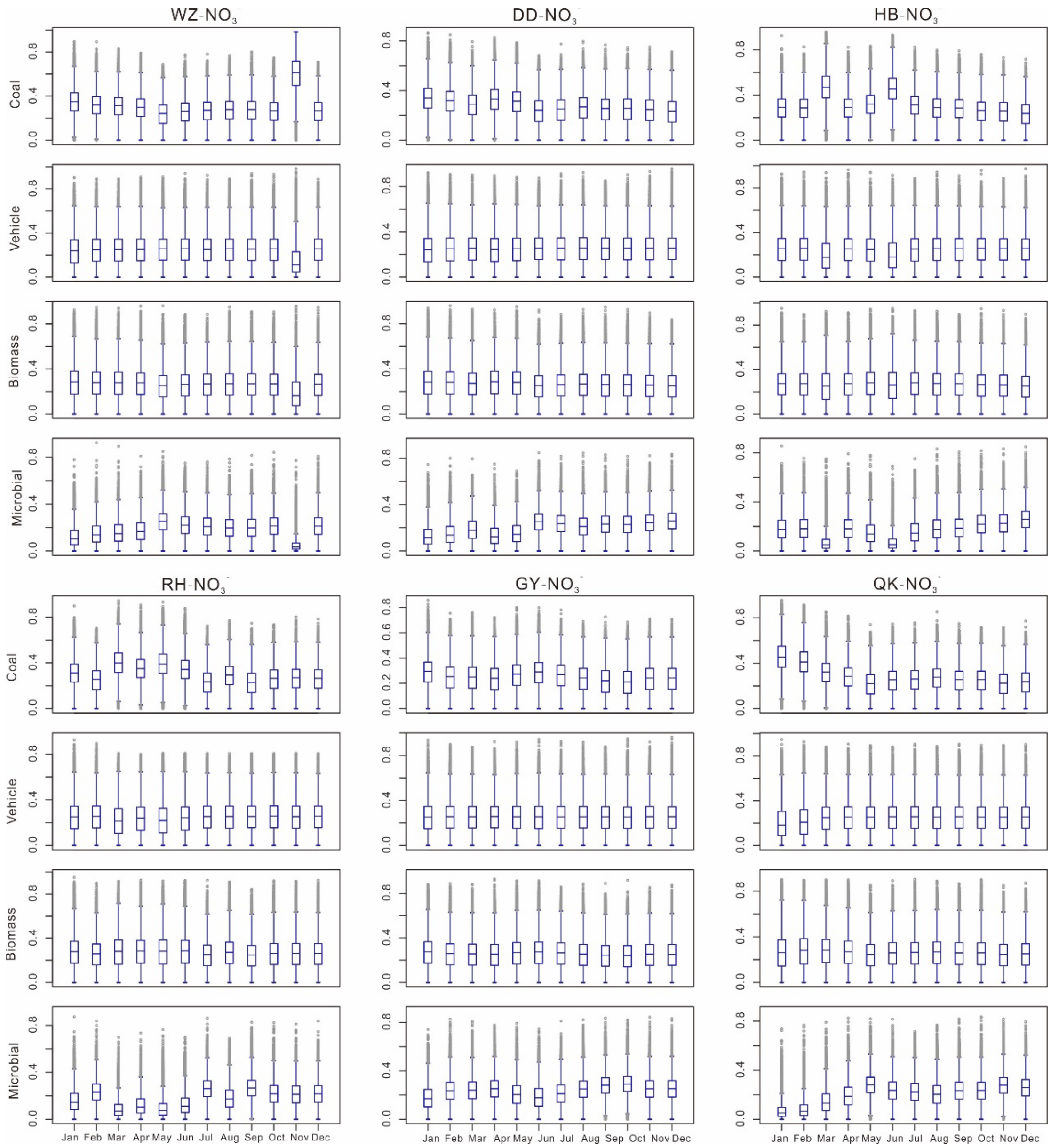

Fig.S4 Seasonally fractional contributions (%) of biogenic soil emission (a), biomass burning (b), coal combustion (c), mobile exhausts (d) to precipitation NO_3^--N at urban (WZ), rural (DD, HB, RH, the green color), town (GY) and wetland (QK) sites, respectively. Grey points are percentage data (n=30000) output from the SIAR model. Each box encompasses the 25th-75th percentiles, whiskers are the 5th and 95th percentiles. The line in each box marks the mean fractional contribution.